THE ONE-DIMENSIONAL FINITE ELEMENT ANALYSIS TECNIQUE FOR REAL-TIME VIBRATION CONTROL OF THIN-STEEL-PLATE

Kimihiko,Sato & Susumu,Torii
Department of Electrical and Electronic Engineering,Musashi Institute of Technology, Tokyo, Japan

ABSTRACT: In conveyance of steel-plates, generation of the crack by friction and vibration becomes a problem. To avoid the problem, the non-contact carrier systems using the attractive force of the electromagnet are used. In these systems, the feedback controls with the sensors are required for stable levitation. In order to reduce the cost of sensors, sensorless control is studied.

In this study, we discuss the analysis technique in the one-dimensional model of a thin-steel-plate. The modeling is reconsidered first to make the modeling error small. Second, the real vibration and the analyzed results of vibration are compared with forced vibration. Then levitating experiment is conducted by independent control and vibration is compared. Finally, the stability of the system is studied.

1 BACKGROUND

Generally, thin steel plates are used in the electric industry, a space industry, the auto mobile industry, and so on. Then, while the products of high quality are required, the demand of quality steel plates such as coated steel plates, surface treatment plates and steel plates that performed high tensionization is also increasing. In the process which manufactures products using steel plates, generally they are conveyed with rollers. However problems, such as peeling of plating and cracks, are arisen by contact friction of steel plates and rollers. As a result, it is necessary to rework steel plates after conveyance, and losses happen in terms of cost or time. Therefore, the magnetic levitation of steel plates which do not have contact is researched.

In this system, feedback control using displacement sensors is needed for stable levitation. Moreover, when flexible steel plates are used in magnetic levitation, they are easy to generate vibration mode and be bended. Furthermore, since the position of loops or nodes changes by vibration mode, devices are required for arrangement of electromagnets. As a solution of these problems, support / vibration control of a steel plate with plural electromagnets is raised. However, the sensors of the same number as electromagnets are required, and it costs at a large-scale conveyance line. In addition since sensing points differ from the magnetic pole parts which are the points of action of power, differences of phases happen, and levitation becomes unstable. Then, the method of reducing the number of the sensors as much as possible is required, which is given the same levitation / conveyance accuracy as the case where sensors are used [(1)]. The real-time vibration analysis technique using FEM (FEM: Finite Element Method) is suggested as one of the method. In this system, the thin steel plate used as the object for levitation is modeled with FEM, and vibration control considered the dynamic vibration state is performed. Thereby, it becomes reducible the number of the sensors. Furthermore, by using FEM, it becomes analyzable at various boundary conditions, and the optimal vibration suppression control can be expected toward vibration which changes every moment.

In This paper, first we compare real vibrations and analysis results by FEM with forced vibration in order to decide the optimal number of element division. Next, by independent control, the phase characteristic and amplitude characteristic of real vibration and analysis result are discussed. Finally, in order to make FEM applied to a magnetic levitation system, the state equation of FEM is developed and the stability on a frequency response is discussed.

2 VIBRATION ANALYSIS BY FEM

2.1 Vibration Analysis Technique Using FEM

Fig.1 is the conceptual diagram of estimated position using the vibration analysis by FEM. In this system displacement z_1 fed back from the gap sensor1 and attractive forces by the electromagnet1 and the electromagnet2 are considered as the input of FEM. Then, vibration generated in the position of the electromagnet2 is analyzed one after another. The analyzed displacement is fed back to an electromagnet2 and sensorless control of the electromagnet2 is carried out. By this system, the constitution of the system which reduces the number of the gap sensors is attained.

First, an analysis program is created based on the equation of motion of the beam in much flexibility (discrete).

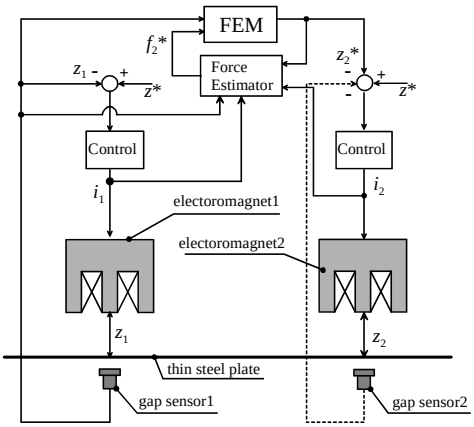

Figure 1. The conceptual diagram of the levitation system using estimated position according to FEM

2.2 Dispersion of Equation of Motion by FEM

The thin steel plate used by this study are length 500 mm, width 100 mm and thickness 0.8 mm. thickness is sufficiently small compared with the length. For the reason, the beam is modeled using assumption of Bernoulli-Euler.

The equation of beam is represented by Bernoulli-Euler as shown in equation (1).

$$M\frac{\partial^2 z(x,t)}{\partial t^2}+CI\frac{\partial^5 z(x,t)}{\partial t\partial x^4}+EI\frac{\partial^4 z(x,t)}{\partial x^4}=f \qquad (1)$$

Here *M*: Mass per unit length (kg/m), *C*: Damping coefficient (Ns/m^2), *I*: Moment of inertia of section (m^4), *E*: Young's modulus (N/m^2), *z*: Amount of displacement (m), *f*: External force (N/m)

The matrix equation of motion calculated by the dispersion model of the beam is shown in equation (2).

$$[M]\{a\}+[C]\{v\}+[K]\{\chi\}=\{F\} \qquad (2)$$

Here [*M*]: Inertia matrix, [*C*]: Damping matrix, [*K*]: Stiffness matrix, $\{a\}$: Acceleration vector, $\{v\}$: Rate vector, $\{\chi\}$: Displacement vector, $\{F\}$: External force vector

The inertia matrix, the damping matrix and the stiffness matrix are shown in equation (3), equation (4) and equation (5). Here *l* (m) is the length per unit element and *m* (kg) is the weight per unit element. From equation (2) displacement is calculated by backward-difference approximation. The equation of displacement is shown in equation (6).

$$[M]=m\begin{bmatrix}\frac{1}{2}&0&\cdots&\cdots&\cdots&\cdots&\cdots&\cdots&0\\0&\frac{l^2}{24}&\ddots&&&&&&\vdots\\\vdots&0&1&\ddots&&&&&\vdots\\\vdots&&\ddots&\frac{l^2}{12}&\ddots&&&&\vdots\\\vdots&&&\ddots&1&\ddots&&&\vdots\\\vdots&&&&\ddots&\ddots&\ddots&&\vdots\\\vdots&&&&&\ddots&\frac{l^2}{12}&\ddots&\vdots\\\vdots&&&&&&\ddots&\frac{1}{2}&0\\0&\cdots&\cdots&\cdots&\cdots&\cdots&\cdots&0&\frac{l^2}{24}\end{bmatrix} \qquad (3)$$

$$[C]=\frac{CI}{l^3}\begin{bmatrix}12&6l&-16&6l&0&0&0&0&\cdots&\cdots&\cdots&\cdots&\cdots&0\\6l&4l^2&-6l&2l^2&0&0&0&0&\ddots&\ddots&&&&\vdots\\-12&-6l&24&0&-12&6l&0&0&\ddots&\ddots&&&&\vdots\\6l&2l^2&0&8l^2&-6l&2l^2&0&0&\ddots&\ddots&&&&\vdots\\0&0&-12&-6l&24&0&-12&6l&\ddots&\ddots&&&&\vdots\\0&0&6l&2l^2&0&8l^2&-6l&2l^2&\ddots&\ddots&&&&\vdots\\0&0&0&0&-12&-6l&24&0&\ddots&\ddots&\ddots&&&\vdots\\0&0&0&0&6l&2l^2&0&8l^2&\ddots&\ddots&\ddots&\ddots&&\vdots\\\vdots&\ddots&\ddots&\ddots&\ddots&\ddots&\ddots&\ddots&\ddots&\ddots&\ddots&\ddots&\ddots&\vdots\\\vdots&\ddots&\ddots&\ddots&\ddots&\ddots&\ddots&\ddots&\ddots&\ddots&-6l&\ddots&0&0\\\vdots&&&&&&0&\ddots&\ddots&-6l&24&0&-12&6l\\\vdots&&&&&&&0&\ddots&\ddots&0&8l^2&-6l&2l^2\\\vdots&&&&&&&&0&0&-12&-6l&12&-6l\\0&\cdots&\cdots&\cdots&\cdots&\cdots&\cdots&\cdots&\cdots&0&6l&2l^2&-6l&4l^2\end{bmatrix} \qquad (4)$$

$$[K]=\frac{EI}{l^3}\begin{bmatrix}12&6l&-16&6l&0&0&0&0&\cdots&\cdots&\cdots&\cdots&\cdots&0\\6l&4l^2&-6l&2l^2&0&0&0&0&\ddots&\ddots&&&&\vdots\\-12&-6l&24&0&-12&6l&0&0&\ddots&\ddots&&&&\vdots\\6l&2l^2&0&8l^2&-6l&2l^2&0&0&\ddots&\ddots&&&&\vdots\\0&0&-12&-6l&24&0&-12&6l&\ddots&\ddots&&&&\vdots\\0&0&6l&2l^2&0&8l^2&-6l&2l^2&\ddots&\ddots&&&&\vdots\\0&0&0&0&-12&-6l&24&0&\ddots&\ddots&\ddots&&&\vdots\\0&0&0&0&6l&2l^2&0&8l^2&\ddots&\ddots&\ddots&\ddots&&\vdots\\\vdots&\ddots&\ddots&\ddots&\ddots&\ddots&\ddots&\ddots&\ddots&\ddots&\ddots&\ddots&\ddots&\vdots\\\vdots&\ddots&\ddots&\ddots&\ddots&\ddots&\ddots&\ddots&\ddots&\ddots&-6l&\ddots&0&0\\\vdots&&&&&&0&\ddots&\ddots&-6l&24&0&-12&6l\\\vdots&&&&&&&0&\ddots&\ddots&0&8l^2&-6l&2l^2\\\vdots&&&&&&&&0&0&-12&-6l&12&-6l\\0&\cdots&\cdots&\cdots&\cdots&\cdots&\cdots&\cdots&\cdots&0&6l&2l^2&-6l&4l^2\end{bmatrix} \qquad (5)$$

$$[\bar{K}]\{\chi_t\}=\{\bar{F}\} \qquad (6)$$

$$[\bar{K}]=\left([M]\frac{1}{\Delta t^2}+[C]\frac{1}{\Delta t}+[K]\right)$$

$$\{\bar{F}\}=\{F\}+[M]\left(\frac{\{\chi_{t-\Delta t}\}}{\Delta t^2}+\frac{\{v_{t-\Delta t}\}}{\Delta t}\right)+[C]\frac{\{\chi_{t-\Delta t}\}}{\Delta t}$$

2.3 Flow of Vibration Analysis by FEM

The flow of an analysis program is shown in Fig.2.

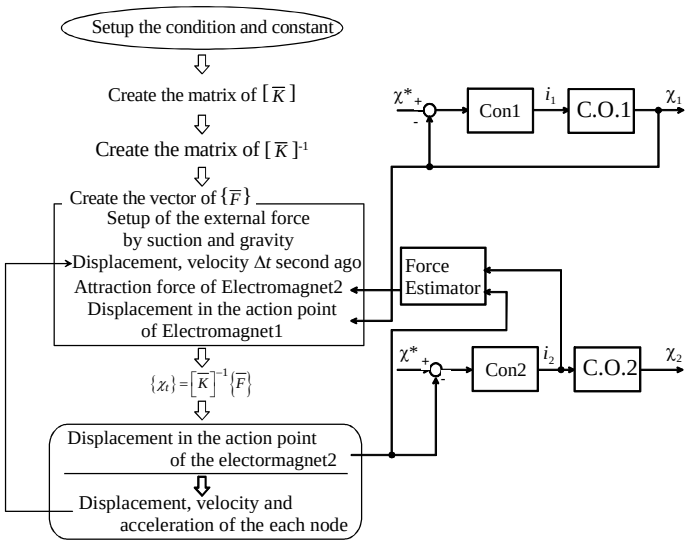

Figure 2. Flow chart of the analysis calculation by FEM

Since the analysis is conducted on real time, it is necessary to reduce the time. Then, the inverse matrix of $\left[\bar{K}\right]$ matrix is determined before the analysis. The initial condition of the analysis sets displacement, speed and acceleration at zero. Moreover, the external force by gravity is considered in addition to the attractive force in the point of action. After $\left\{\bar{F}\right\}$ vector is calculated, displacement is estimated using equation (6). The calculation performed within a control cycle becomes from calculation of $\left\{\bar{F}\right\}$ to calculation of displacement $\left\{\chi_t\right\}$.

3 STUDY OF REAL VIBRATION AND ANALYSIS RESULT

3.1 Comparing Study of Real Vibration and Analysis Result by Forced Vibration

Fig.3 is the model of the test prototype using a vibrator.

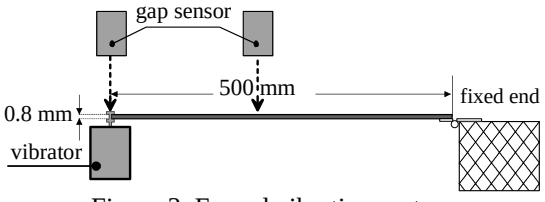

Figure 3. Forced vibration system

Vibration of amplitude 0.5 - 1 mm and frequency 5 Hz - 15 Hz is given by a vibrator. The number of the element divisions is set to 120,150,200, and the vibration of the beam is analyzed. The frequency characteristic of the analysis result on real vibration in the central point (250 mm) of a beam is shown in Fig.4.

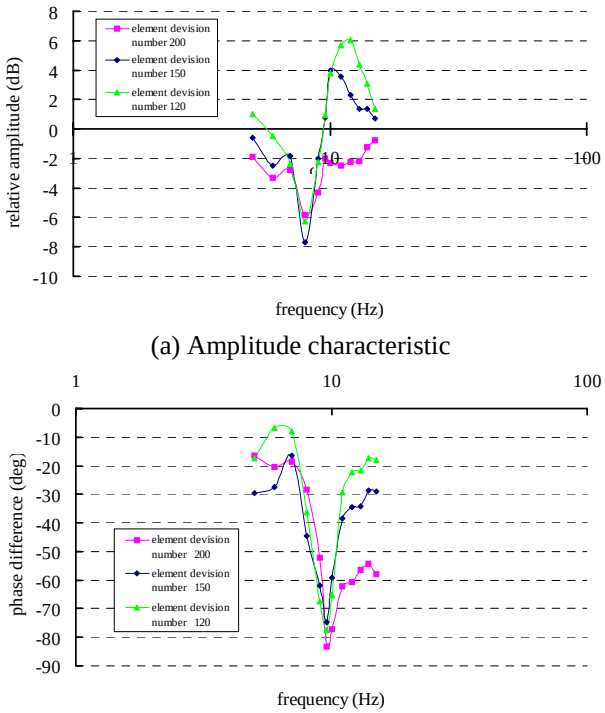

(a) Amplitude characteristic

(b) Phase characteristic

Figure. 4. The frequency characteristic of the analyzed result in real vibration

From Fig.4, an amplitude characteristic has a resonating point in 8 Hz, and phase characteristic has a resonating point in 9.6 Hz. In an amplitude characteristic, it can check that the result of the analysis is intense change with few divisions. The phase characteristic with 200 element divisions has late of the phase about 58 deg after 9.6Hz. It is thinkable that the analysis time is long toward the velocity of the wave between elements. In each number of the divisions, the rate of the analysis time toward the velocity of the wave between elements is 120:150:200= 1:1.5:2.6. We confirmed that a difference of phase characteristics also had an alteration of the mostly comparable ratio.

When the accuracy of the analysis and the real vibration toward change of the number of the element divisions are compared, gain characteristics and phase characteristics have a relation of the trade-off. Therefore, in consideration of mounting to a magnetic levitation system, it is necessary to determine the optimal number of the divisions. When FEM is used as substitution of a sensor, it considers that a difference of phase characteristics works attractive force for reverse, and makes levitation unstable. For the reason if the number of the divisions is determined taking notice of phase characteristics, it will be thought that 120 divisions with few differences of a phase is the optimal.

3.2 Levitating Experiment by Independent Control

The levitating system by independent control is shown in Fig.5.

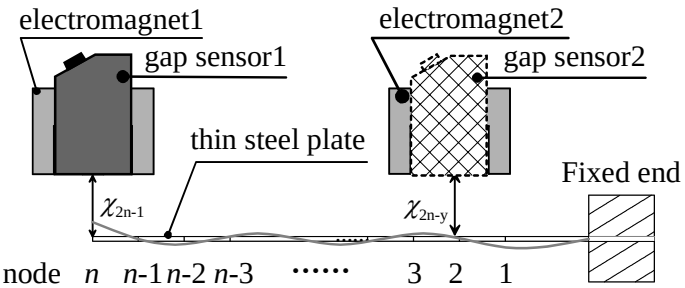

Figure 5. Vibration analysis model of thin steel plate

An electromagnet2 and a sensor2 are installed in the center of a beam, and a levitating experiment is conducted by independent control. It performs comparing of real vibration and analysis results generated at the time of levitation when changing a control cycle and the number of the element divisions.

In this experiment, the fiducial point of a levitating gap shall be 2.5mm. Levitation of thin steel plate was examined that stable levitation was done by 0.8msec or less. However, stability was low and became vibration-like at 1.2msec. It is thought that the cause is the delay time by means of a time sampling. The phase differences and the amplitude differences in each number of the element divisions are shown in Fig.6.

From Fig.6 (a), it finds that when control cycles are 1.2msec, the phase difference of 72deg is generated, and phase difference becomes small as the number of the element divisions is decreased. Like Section 3.1, it is founded on the relation of the analysis time to the speed of the wave which transmits between elements. Fig.6 (b) shows that the amplitude difference at the time of control cycle 1.2msec is large. A damping coefficient can be considered as one of the cause of this. The damping coefficient used this examine is the value got by free vibration. However, it thinks that the damping coefficient changes depending on vibration frequency. We think that the effect is generated at control cycle 1.2msec.

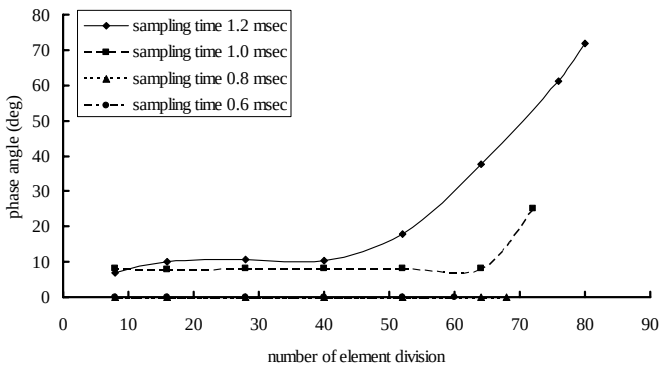

(a) Phase characteristics

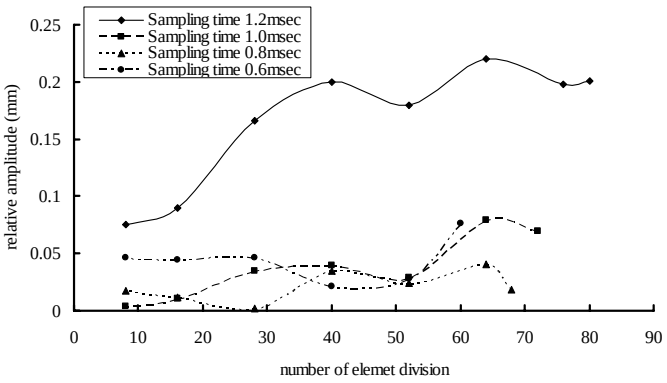

(b) Amplitude characteristic

Figure 6. Comparing of real vibrations and analysis results generated at the time of levitation

At the time of control cycle 0.8msec, phase difference is 0 deg and an amplitude difference is also less than 0.05mm, and it is the closest to real vibration. However, 0.2mm gap length had happened as offset. Offset of each control cycle is shown in Table 1. As shown in table 1, offset became such a big value that a control cycle is long.

Table1. Gap length's offset in control cycles

control cycle [msec]	0.6	0.8	1	1.2
gap length's offset [mm]	0.2	0.2	0.4	0.6

From Fig.6, it considers about phase characteristics that the analysis time can be decreased within 10 deg by making it quick more than double from the speed of the wave which transmits between elements.

4 STABILITY OF MAGNETIC LEVITATION SYSTEM USING FEM

4.1 Securing of Controllability and Observability of Magnetic Levitation System

In order to fit FEM to the control system, the equation of motion dispersed to the *n* element *n* node is expressed with the state equation.

The state equation and output equation of equation (2) turn into equation (7). Here considered as state vector is **X** (4*n* by 1), system matrix is **A** (4*n* by 4*n*), control matrix is **B** (4*n* by 2*n*), control input is **u** (4*n* by 1) and observation matrix is **C** (1 by 4*n*).

$$\left.\begin{aligned}\dot{\mathbf{X}} &= \mathbf{AX} + \mathbf{Bu} \\ \mathbf{y} &= \mathbf{CX}\end{aligned}\right\} \tag{7}$$

$\mathbf{X} = \begin{bmatrix} \{x_{(2)}\} & \{x_{(1)}\} \end{bmatrix}^{\mathrm{T}}$, $\mathbf{C} = [0 \quad \mathbf{D}]$, $\mathbf{u} = \{f\}$

$\{x_{(2)}\} = \{\dot{\chi}(t)\} = \{\dot{x}_{(1)}\}$, **D**: Position of a estimating point, $\mathbf{A} = \begin{bmatrix} -\mathbf{M}^{-1}\mathbf{C} & -\mathbf{M}^{-1}\mathbf{K} \\ \mathbf{I} & 0 \end{bmatrix}$, $\mathbf{B} = \begin{bmatrix} \mathbf{M}^{-1} \\ 0 \end{bmatrix}$

The electromagnet1 and the gap sensor1 of Fig.5 are installed in the free end of a one end fixed beam, and an electromagnet2 is installed in another points. In this study the primary mode and the secondary mode are controlled.

Since the controllability and the observability of the magnetic levitation system are secured, it is necessary to avoid the node of the secondary mode and to install an electromagnet. Then, the modal analysis of the levitating object is done and the secondary mode is hold. The vibration mode vector by the modal analysis in case that the number of the element divisions is 60 is shown in Fig.7.

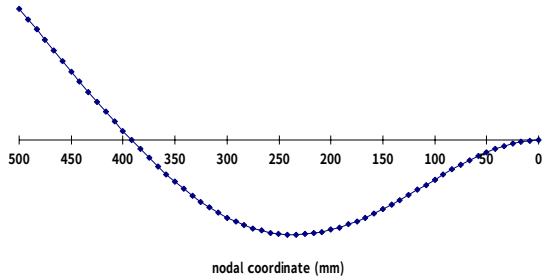

Figure 7. Vector wave in the secondary mode

From Fig.7, the node of the secondary mode arises from a fixed end near 390mm (node number 47). Therefore, we consider that the controllability and the observability at the time of installing an electromagnet and a sensor in the node number 47.

As conditions which check the controllability and the observability, power *f* is given only to the node (node 47) in the secondary mode, and the external force by gravity is disregarded. Coordinate transformation of the equation (7) is done using the coordinate transformating matrix **T**, and it develops as the diagonal canonical form. The equation developed to the diagonal canonical form is shown in equation (8) [6]

$$\left.\begin{aligned} \dot{\mathbf{Z}} &= \tilde{\mathbf{A}}\mathbf{Z} + \tilde{\mathbf{B}}\mathbf{u} \\ y &= \tilde{\mathbf{C}}\mathbf{Z} \end{aligned}\right\} \tag{8}$$

$\tilde{\mathbf{A}} = \mathbf{T}^{-1}\mathbf{A}\mathbf{T} = \mathrm{diag}(\lambda_1 \quad \lambda_2 \quad \cdots \quad \lambda_3)$

$\tilde{\mathbf{B}} = \mathbf{T}^{-1}\mathbf{B} = [\beta_1 \quad \beta_2 \quad \cdots \quad \beta_3]^{\mathrm{T}}$

$\tilde{\mathbf{C}} = \mathbf{C}\mathbf{T} = [\theta_1 \quad \theta_2 \quad \cdots \quad \theta_3]$

The block diagram of equation (8) is shown in Fig.8.

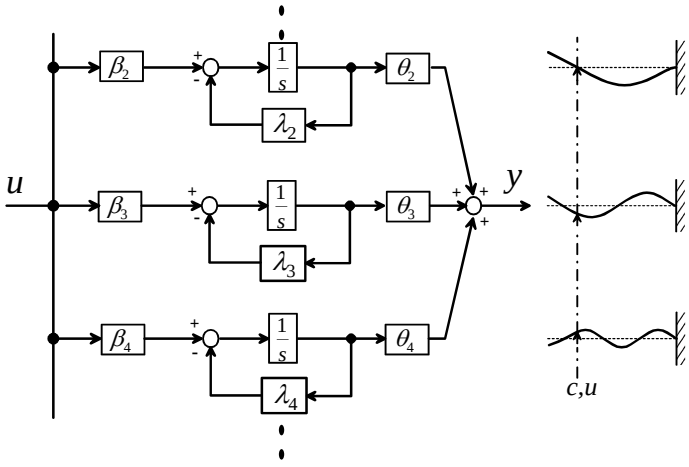

Figure 8. Secure of the controllable and observable by the diagonal canonical form

The block diagram of each vibration mode is given with a subsystem like Fig.8, and it becomes improper control and improper observation at the time of β_n=0, θ_n=0. From equation (8), the controllability and the observability are discussed by the case where an electromagnet or a sensor is installed in the node of the secondary mode or the other points. The calculation result of β_n and θ_n obtained by MATLAB is shown in Table 2.

Table.2 Evaluation of the controllable and observable in the secondary mode

Position of electro magnet and sensor	β_n	θ_n
node number 30	-406.2	-1.6E-02
node number 47 (nodal point)	-0.7	-2.6E-05
node number 48	39.4	1.5E-03
node number 57	432.7	1.7E-02
node number 60	568.8	2.2E-02

From Table 2, when an electromagnet and a sensor are installed in a node, it is set to $\beta_n \simeq 0$ and $\theta_n \simeq 0$, and it becomes improper control and improper observation. The controllability and the observability of the system are secured by avoiding a 390mm point from a fixed end and installing an electromagnet and a sensor.

4.2 Discussion of Stability of FEM Suited to Magnetic Levitation System

In order to make the equation (7) applied to the magnetic levitation system of Fig.5, the state equation is developed.

Equation (7) is divided into known variables and strange variables, and it develops to simultaneous linear equations. 4*n*-1 variable contained in the state variable of equation (7) is a known value got from a sensor. For the reason, a corresponding line and sequences are separated from equation (7), and it is made a matrix small one dimension. The attractive force of an electromagnet is linearized by approximation neighborhood the position of equilibrium, and becomes equation (9). Next, in order to carry out control input to one input, the external force by the gravity contained in an input {*f*} is separated. The equation which developed the equation (7) is shown in equation (10).

$$f_{2n\text{-}y} = \frac{2kI^2}{\chi_{2n-y}^3}\Delta\chi_{2n\text{-}y} - \frac{2kI}{\chi_{2n-y}^2}\Delta i \tag{9}$$

$$\dot{\mathbf{X}}' = \mathbf{A}'\mathbf{X}' + \mathbf{B}''\, f_{2n\text{-}y} + \mathbf{a}x_{(1)2n-1} + \mathbf{b}f_{2n-1} + \mathbf{B}'\mathbf{f}_{mg} \tag{10}$$

$\mathbf{X}'$: $\mathbf{X}$ vector of (4n-1 by 1)

$\mathbf{f}_{mg}$: external force by gravity

a: column vector separated from **A**, **b**: column vector separated from **B**, $\mathbf{A}'$: **A** vector of (4n-1 by 4n-1), $\mathbf{B}'$: **B** vector of (4n-1 by 2n-1), $\mathbf{B}'' : \mathbf{B}' \times \mathbf{D}^{T}$, $\mathbf{D}'$: **D** vector of (1 by 2n-1)

From equation (10), the block diagram which applied FEM to the magnetic levitation system is shown in Fig.9.

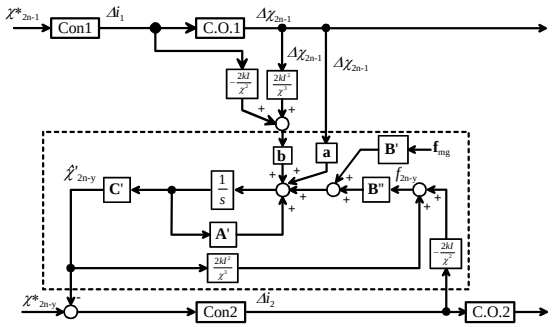

Figure 9. Block diagram of a magnetic levitation system using FEM

From Fig.9, the magnetic levitation system of this study needs to input the information from a gap sensor into FEM, and the minor loop which the gain cannot adjust generates it. For the reason, it is necessary to check the effect by a minor loop. Accordingly, the effect is checked from the transfer function of the FEM area. At this point, from fig.9 it is considered that the input from an electromagnet1 is the external force to FEM. The block diagram of the FEM area which disregarded external force is shown in Fig.10, and the frequency response calculated from Fig.10 is shown in Fig.11.

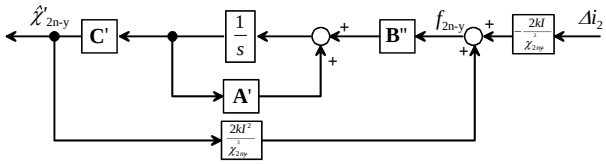

Figure 10. Block diagram of FEM which disregarded external force

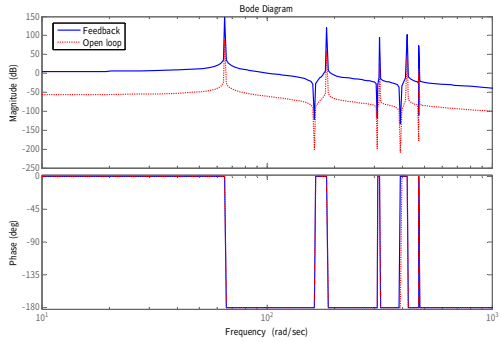

Fig 11. Comparing of frequency response between open loop and feedback

From Fig.11, when open loop and feedback are compared, it becomes the wave which is shifted a fixed multiple. From this result, the FEM system of Fig.10 can be considered that there is almost no effect of a current input part, and the effect of feedback from $\chi_{2n\text{-}y}$ is dominant. Therefore, displacement from the electromagnet1 disregarded as external force is set as the input of FEM, and it examines again in consideration of all the current input parts as external force.

The block diagram of the FEM area shown in Fig.9 becomes Fig.12. Then, a new system matrix is created by summarizing the parallel portion of Fig.12. The block diagram which summarized Fig.12 is shown in Fig.13.

At this point, a control matrix constitutes equation (11).

$$\mathbf{B}_a = \mathbf{a} + \frac{2kI^2}{\chi^3}\mathbf{b} \tag{11}$$

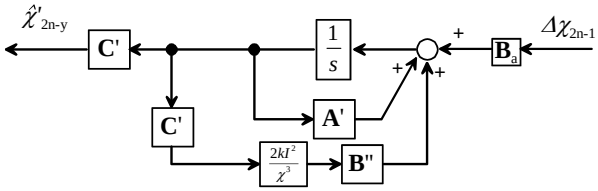

Fig 12. Block diagram of FEM at the time of considering displacement of an electromagnet 1 as an input

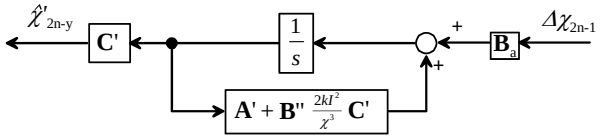

Fig 13. Block diagram of FEM which compounded the parallel part

From Fig.13, when an electromagnet1 is considered as an input, it becomes a system without a minor loop. This is because that it was collected as a system matrix like Fig.13 since the current input of the electromagnet2 was treated as external force. The above result shows that the system of the minor loop of Fig.9 does not show effect to a frequency response at the position directive.

5 CONCLUSION

In this paper, we showed the vibration control using FEM as one of the techniques of sensorless control. Then, by forced vibration, the frequency characteristic of the real vibration and the analysis results was discussed, and it was presupposed that 120 divisions is appropriate. Moreover, it checked that the analysis result at the time of control cycle 0.8msec was the closest to real vibration by independent control. Finally, discussion about the stability of the state equation of FEM made applicable to a magnetic levitation system was performed. As a result, when a current input is treated as external force, we think that it is a stable system by the frequency characteristic.

In the future, sensorless levitation using the analysis result obtained by FEM is carried out. Then, stable levitation is aimed at by designing vibration suppression control. Besides, study about the effect on levitation accuracy is performed by changing an analyzing point.

6 REFERENCES

M.Huruhasi 1994. *Self-sensing Active Vibration Control of a Thin Steel Sheet*, The japan society of mechanical engineers C, Vol.60, No.578:pp.3308-3313

M.Sase & S.Torii 2002. *Magnetic levitation control with real-time vibration analysis using finite element method.* International Journal of Applied Electromagnetics and Mechanics. Vol.13, Nos.1-4: pp.129-136

A.tanaka, S.Torii 2004. *Magnetic levitation control with real-time and fewer sensors finite element method*. International Journal of Applied Electromagnetics and Mechanics. Vol.19, Nos.1-4: pp.679-683

H.Togawa 1975. *Vibration analysis by FEM*, Science company: pp.1-12

K.Nonami & S. Kobayasi 1975. *Controllability and observability in flexible rotor-magnetic bearing systems*, The japan society of mechanical engineers C, vol.56 , No.528: pp.2065-2071

A.Ngamatu. Modal 1996. analysis and control of sound ・ vibration, Corona company: pp.193-201